



HAL
open science

Fiducial Point Estimation Solution for Impedance Cardiography Measurements

Olev Martens, Margus Metshein, Anar Abdullayev, Benoit Larras, Antoine Frappé, Antoine Gautier, Maryam Saeed, Deepu John, Barry Cardiff, Andrei Krivosei, et al.

► **To cite this version:**

Olev Martens, Margus Metshein, Anar Abdullayev, Benoit Larras, Antoine Frappé, et al.. Fiducial Point Estimation Solution for Impedance Cardiography Measurements. IEEE I2MTC 2022, May 2022, Ottawa, Canada. 10.1109/I2MTC48687.2022.9806596 . hal-03760061

HAL Id: hal-03760061

<https://hal.science/hal-03760061v1>

Submitted on 24 Aug 2022

HAL is a multi-disciplinary open access archive for the deposit and dissemination of scientific research documents, whether they are published or not. The documents may come from teaching and research institutions in France or abroad, or from public or private research centers.

L'archive ouverte pluridisciplinaire **HAL**, est destinée au dépôt et à la diffusion de documents scientifiques de niveau recherche, publiés ou non, émanant des établissements d'enseignement et de recherche français ou étrangers, des laboratoires publics ou privés.

Fiducial Point Estimation Solution for Impedance Cardiography Measurements

Olev Martens

Tallinn Univers. of Technol., Estonia
olev.martens@taltech.ee

Margus Metshein

Tallinn Univers. of Technol., Estonia
margus.metshein@taltech.ee

Anar Abdullayev

Tallinn Univers. of Technol., Estonia
anar.abdullayev@taltech.ee

Benoit Larras

Univ. Lille, CNRS, Lille, France
benoit.larras@junia.com

Antoine Frappe

Univ. Lille, CNRS, Lille, France
antoine.frappe@junia.com

Antoine Gautier

Univ. Lille, CNRS, Lille, France
antoine.gautier@junia.com

Maryam Saeed

University College Dublin, Ireland
maryam.saeed@ucdconnect.ie

Deepu John

University College Dublin, Ireland
deepu.john@ucd.ie

Barry Cardiff

University College Dublin, Ireland
barry.cardiff@ucd.ie

Andrei Krivošei

Tallinn Univers. of Technol., Estonia
andrei.krivosei@taltech.ee

Paul Annus

Tallinn Univers. of Technol., Estonia
paul.annus@taltech.ee

Marek Rist

Tallinn Univers. of Technol., Estonia
marek.rist@taltech.ee

Abstract—ICG (impedance cardiography) is in parallel to ECG (electrocardiography) an important indicator of the functioning of the heart and of the overall cardiovascular system. Adding the ICG to ECG measurement functionality into the wearable devices improves the quality of health monitoring, as the ICG reflects relevant hemodynamic parameters (informative time intervals, but also the stroke volume and cardiac output and their variability). The most challenging task of the ICG signal processing is to extract the key points B, C, X of the cardiac period – start, peak-location, and value at this point and the end of the LVET (left ventricular ejection time) sub-period in the cardiac cycle. A novel block diagram and analog implementation of it has been proposed, analyzed, and discussed, with discussion of the benefits of the proposed solution. The proposed solution enables developing of relatively simple very power-efficient solutions, monitoring the ICG values of the person with smart and efficient data acquisition and processing.

Index Terms—impedance cardiography (ICG), electrical bio-impedance (EBI)

I. INTRODUCTION

ECG (electrocardiography) and ICG (impedance cardiography) are both important means to monitor the cardiac activity and heart condition [1]. While ECG (indicating the electrical signals of the heart) has a long history from the end of the 1800-s, then ICG (showing physical work of the heart and reflecting hemodynamical parameters) has been used from the 1960-s [2]. With help of ICG, it is possible to estimate additionally to heart rate (HR) and its variation (HRV), the

efficiency of blood pumping –cardiac output (CO) and stroke volume (SV), but also various timings, e.g. left ventricular ejection time (LVET) and pre-ejection period (PEP) [3].

Portable solutions have been developed to monitor these and other parameters [4]. Example waveforms of the ICG signals (with ECG signal in parallel) are shown in Fig. 1 [4]. On the plots, the ECG signal is shown for reference, together with the impedance (Z) signal and the first derivative (dZ/dt), as the actual “ICG signal” [2]. While the ECG signal is characterized by the QRS complex (Fig. 1), for ICG the following key points and time intervals are typically used to characterize the cardiac periods [2], [4]:

- B - Opening of the aortic valve;
- C - Maximum systolic flow;
- X - Closing of the aortic valve;
- Y - Closing of the pulmonary valve;
- O - Opening of the mitral valve;
- PEP - Pre-ejection period;
- LVET - Left ventricular ejection time.

For ICG most relevant points are B, C, X -allowing to estimate the LVET, CO, and SV [3].

Historically ICG impedance waveforms have been measured involving the whole thorax [2] (including the heart and the lungs) into the measurement signal path. So, a simple wearable belt can be used for measurement setup, to acquire ECG and ICG signal simultaneously [5]. Alternatively, the cardiac waveforms can be obtained from other places, e.g. by measuring from the wrist [6]–[8], being probably the preferred variant for wearable devices (to implement the devices in the form of smart watches).

This work was supported by EU Regional Development Fund (Mobilitas+ project *Mobera20* and Estonian Centre of Excellence in ICT Research EXCITE TAR16013), Estonian Research Council (grant PRG1483), Irish Research Council and French Research Agency project ANR-19-CHR3-0005-01.

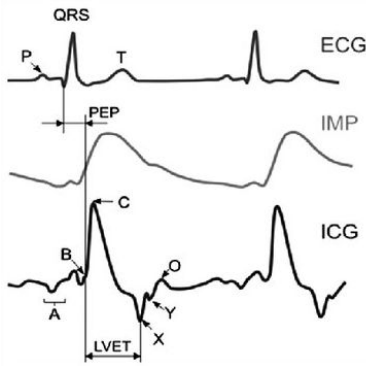


Fig. 1: Typical patterns of the ECG and ICG waveforms [4]

Current paper focuses on the estimation of hemodynamic feature points by using the signal of ICG, gained e.g. from the wrist. A novel solution, directed by the “edge computing” principles, is proposed, analyzed and compared to the closest solution described in designated literature. The presented work is expected to guide closer to the “on-site” estimation and analyze of bio-signals and throughout, innovative solutions in wearable technologies.

II. POSSIBLE ALGORITHMS TO EXTRACT THE KEY POINTS OF ICG

The key- (fiducial) points B, X, C are typically (e.g. in [3]) defined as following - the C is the most positive peak (maximum) value in the ICG signal (dZ/dt) and can be found as a global extremum in some reasonable (corresponding e.g. to an expected pulse period) sliding time window. Additionally a threshold can be applied- only the positive extremums over e.g. 50% of the overall signal maximum level are taken into account. For determining the B-point various approaches have been proposed. Most typically the first zero-crossing of the ICG to the left from the C-point is used [3], [4], [9], [10]. The same approach is used in the proposed solution. As for algorithm, the determining of the B-point strategy can be rephrased as “fixing the last zero crossing of the ICG signal before the C-point”. Alternatively the B-point has been suggested to take as some local minimum [2] further left from the zero-crossing (“below the zero”), so giving little bit increased value for LVET interval (and related CO and SV values). As another alternative, it has been proposed to move the B-point by applying instead of zero-crossing the crossing at the 15% level between the base-line (close to zero, in practice) and peak value [11].

For determining the X-point most often the global minimum (negative extremum) of the ICG signal, between every C-to-(next) C interval is considered [4], [9], [10]. For the current solution this approach is used, up to further reconsideration.

A. Problem statement

Wearable solutions exist for monitoring of the ICG and ECG (or solely ICG) signals ([4], [12], [13]). In known solutions the wearable part of electronics performs typically only the signal

acquisition and first preliminary signal conditioning - detecting of AC carrier of the impedance signal, filtering and digitizing (e.g. with 12-16 bits and at 200 Hz rate). Detecting of AC carrier of the bio-impedance signal is preferably performed by synchronous detection (known also as *lock-in technique* [14]) giving better performance in the presence of noise, disturbances and artifacts. Also bandpass (combination of highpass and lowpass) filtering is required before further signal processing. The highpass filtering is needed to remove the base component of the bioimpedance Z_0 to process only relatively tiny variations ΔZ of the total impedance $Z = Z_0 + \Delta Z$. Lowpass filtering is needed for several reasons- to fulfill the Nyquist criteria before digitizing, to suppress various noise of acquired signals and sensitive front-end electronics, but also to smooth the output signal of the (e.g. *lock-in*) detector.

Further the digitized data stream with the waveform(s) is transmitted by wireless (e.g. Bluetooth) connection to the computer, tablet, smartphone or some other device for feature extraction (starting from determining the characteristic points of ICG) and further analysis, determination of various (hemodynamic) parameters for presentation (and optionally logging) of the waveforms and displaying of the determined values.

Such solutions, with high-rate high-resolution signal sampling analog-to-digital conversion with sophisticated mathematical operations take much energy and involve sophisticated circuitry, not allowing to offer low-cost low-power simple wearable monitor devices.

Much more reasonable alternative, proposed in the current paper, is to use the “edge computing” principles, extracting the main information just near the sensor, “*at first possibility*”, still in the analog signal domain. For possible implementation of the cardiac activity (or cardiorespiratory, as ICG is reflecting also the lung activity [15]) monitoring device into the smart chip, with local artificial intelligence (AI) is clearly beneficial. The chip has to be low-power with simple and robust enough algorithms. One approach is to make much of the signal processing in the analog and mixed electronics part, acquiring the sparse filtered samples of the bioimpedance only at the characteristic points, starting with B, C, X-points. The time intervals for these points can be measured simply by digital counters and values sampled at these time instances to be digitized, by relatively slow (e.g. by simple integrating type) ADC, based again on counting of some digital clock ticks.

In addition, as background comment, solutions for generic low power systems with non-uniform sampling, event-driven [16] and combined peak and level-crossing sampling schemes [17] have been proposed by various researchers.

B. About known solutions

While there are several papers describing the locations (and their finding strategies) of these fiducial points, only one example (MatLab) software toolbox has been found for determining of these points (“A Biosignal-Specific Processing Tool”, described by the authors of this tool in [3]). Furthermore, no practical implementations such as an analog or digital hardware or even embeddable (e.g. C-code) solutions have

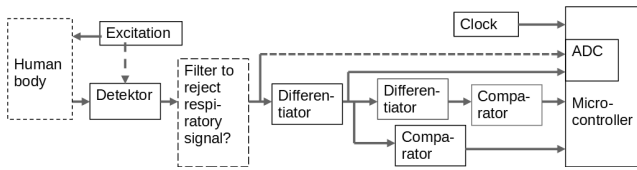


Fig. 2: Solution by B. Sramek [18]

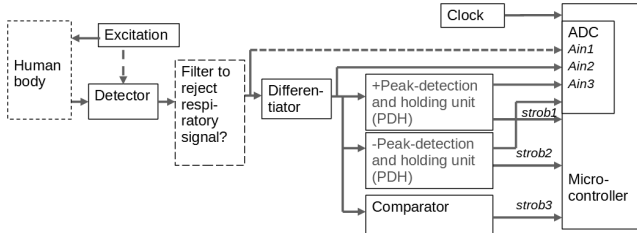


Fig. 3: Proposed solution

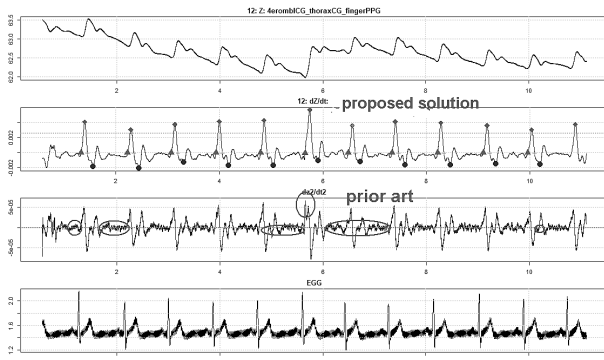


Fig. 4: Block diagram level simulation, prior solution vs proposed

been found by authors of this paper for estimating the key points of ICG.

Still, an US patent of B. Sramek [18] is disclosing partly similar approach (on the block diagram level) to the solution, proposed in the current paper. If to compare the solution of Sramek (Fig. 2) and the proposed solution (Fig. 3), the second differentiator and the second comparator are changed to peak-detectors, being less sensitive to the noise, as shown below. As expected, the simulation example with real ICG signal gives for the prior solution [18] much more false signals, compared with the proposed solution, in detecting the key points of ICG signal, as shown in the Fig. 4.

III. PROPOSED SOLUTION

A. Block diagram of the proposed solution

The more specific block diagram of the proposed solution is shown in the Fig. 5. The solution includes the excitation source (typically 10-100 kHz sinewave signal is used) and pickup of the response signal, which is converted by a signal (typically synchronous) detector (SD) to the bio-impedance Z signal. Typically module or real part of the complex Z is used. Also asynchronous detector can be considered [4] by simplicity reason.

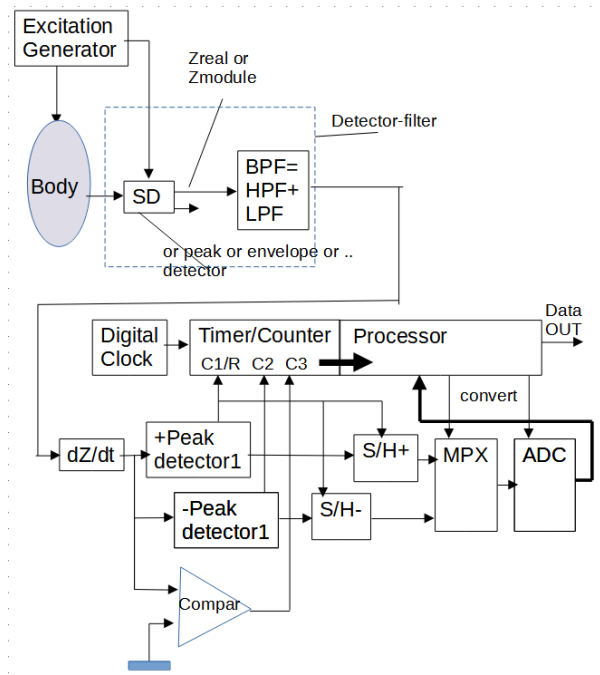


Fig. 5: Block diagram of the proposed solution

This part of the AC excitation and AC detector solution is not shown and analyzed in the solution, as standard solutions, offered also by the authors previously, can be used [14].

Further the high and low-pass filtering and taking of the first derivative (dZ/dt) are applied to extract the ICG signal. The ICG signal is then applied to “+peak” detector and “-peak detector” to follow the positive and negative peaks (extremums) and the comparator (“Compar”) zero-crossings of the ICG signal. Peak detectors are designed in the way, that at the “event” time instance (“+peak”, “-peak” or comparator “zero-crossing”) the events are triggered and strobe signals are generated for digital counter (timer) and to control the sample-and-hold (S/H) units to fix the analog values at key points for further analog-to-digital (AD) conversion. The C-point timer (“+peak”) is fixed at the C1 (C1/R) input of the timer/counter, the X-point count at the C2 input and B-point and C3. Also the “C-point” (“+peak” event), after copying the counts for C1, C2, C3 inputs, resets the timer (by R-input of the C1/R). Also the strobe pulses are generated by peak detectors to control the sample-and-hold units (S/H+ for C- and S/H- for B-point amplitudes). As there will be one (for C-point) or two values (for C- and X-points) to be sampled and AD-converted per cardiac period, the ADC can be reasonably simple, e.g. of counter (timer) based single-slope integrating type.

B. An implementation example of the proposed solution

The schematics of the proposed solution is shown in the Fig. 6. The schematics (made in TINA simulation environment of Texas Instruments (Dallas, TX, US)) include the input signal (generator) V_{ain1} , where the actually (from the wrist) acquired bio-impedance signal is used (as converted to WAV-

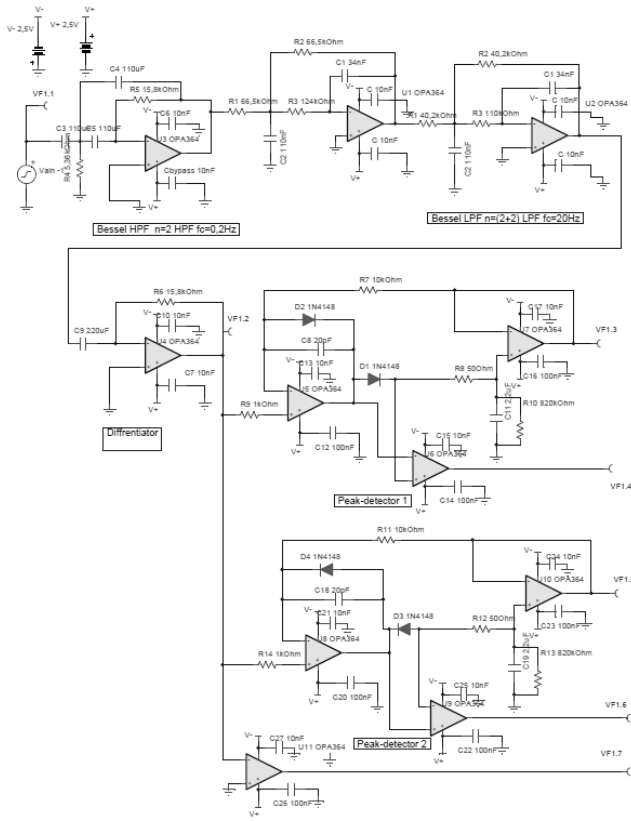


Fig. 6: An implementation example of the proposed solution

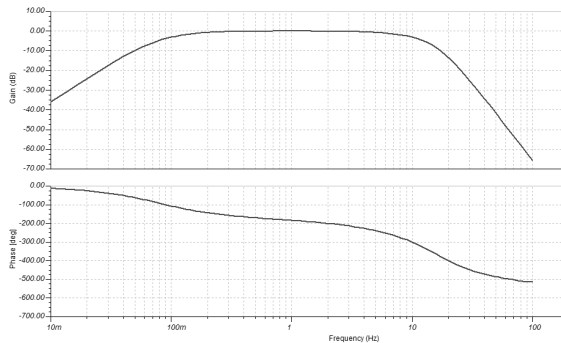


Fig. 7: Frequency response of the filter part

file). The op-amps U1-U3 from first the 2-nd order highpass filter ($f_c=0.1\text{Hz}$) and two 2-nd order lowpass filter-stages ($f_c=10\text{Hz}$), all of Bessel type.

The plot of the overall filter frequency response (magnitude and phase) is given in the Fig. 7. After the differentiator (U4) there are “+peak” and “-peak” detectors to “catch” the C- and X-points. The difference in the implementation of the “+peak” and “-peak” is only in reversing the diodes. The simplified “+peak”-detector is depicted in the Fig. 8. The idea of the peak detector implementation can be a simple “diode-and-capacitor” based circuit, put into the negative feedback path of the op-amp. Also, the voltage drop on the diode can (e.g. through the comparator) generate the strobe pulse, the closing

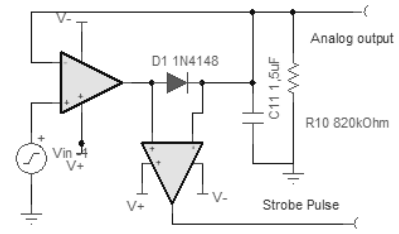


Fig. 8: An example implementation of the peak detector

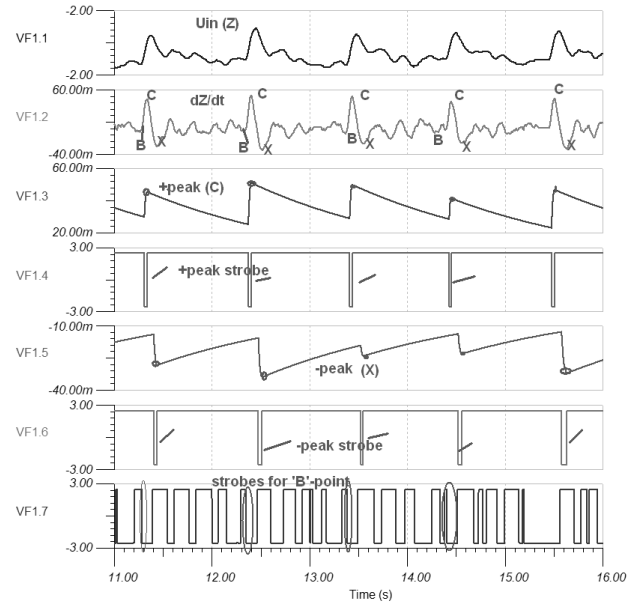


Fig. 9: Waveforms of the proposed solution

of the diode edge shows, that the peak has been acquired and can be “latched” for further processing, as well as in time domain, as well as by its amplitude value. The comparator U11 generates from zero-crossings of the dZ/dt signal the strobe pulses for B-point location. The additional logic is needed, to use the last pulse before the C-point see the VF1.7 curve into the Fig. 9.

For actual CMOS implementation of the peak detectors various solutions have been proposed [19]–[21].

Some waveform curves of the example implementation from LT-Spice simulations are given in the Fig. 9:

- VF1.1 - acquired impedance signal Z (real-life signal acquired from the wrist);
- VF1.2 - signal after filtering and differentiator (dZ/dt);
- VF1.3 - “+peak” signal (for the C-point);
- VF1.4 - strobe signal for the “+peak” signal;
- VF1.5 - “-peak” signal (for the X-point);
- VF1.6 - strobe signal for the “-peak” signal;
- VF1.7 - strobe signals for the B-point (zero crossing of dZ/dt) - the last strobe used at the “+peak” (C-point) event;

C. Comparison with previous solutions

In the papers [22], [23] some estimations of the correctly found fiducial points have been given, being on the level of the 90% or even less. Still, the number of correctly found points depend much on the quality and strength of the signals and how sophisticated signal processing is used, compared to the proposed simple mostly analog (and potentially low-power) signal processing.

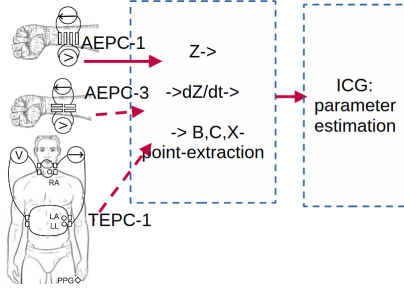


Fig. 10: Measurement setup

The proposed solution is suitable also for weak signals, acquired from the wrist (compared with much stronger signal amplitude from the chest) – see the measurement setup in the Fig. 10. The measurement setups TEPC-1, AEPC-1 and AEPC-3 have been discussed in the paper [24].

Estimation of the correctly found X-X, B-B and C-C time intervals have been carried out in simulations (with real-life signals) for the proposed solution vs the previous solution [18]. The simulation plots are shown in the Fig. 11 (from up to down – original impedance signal Z , first derivative dZ/dt (with fiducial points found by the proposed approach), the second derivative d^2Z/dt^2 (with fiducial points found by the previous method), and finally the ECG waveform).

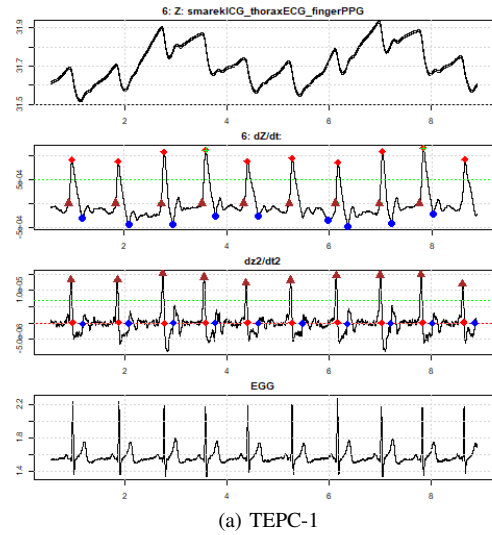
The results of the falsely detected fiducial points (time intervals) has been given in the Table I for the proposed and in the Table II for the previous solution, showing just for weak (wrist) signals significantly improved fiducial point determination.

TABLE I: Number of falsely detected fiducial points for the proposed solution

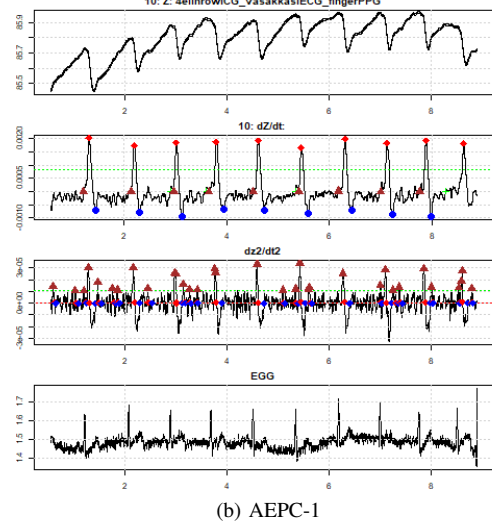
No	Conf	Total periods	B-B errors	C-C errors	X-X errors	Total errors
1	TEPC-1	33	0	0	0	0
1	AEPC-1	20	0	0	1	1
1	AEPC-3	20	0	0	0	0

TABLE II: Number of falsely detected fiducial points for the previous solution

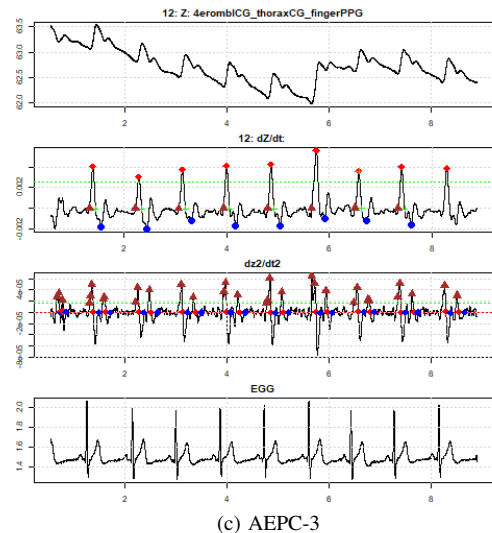
No	Conf	Total periods	B-B errors	C-C errors	X-X errors	Total errors
1	TEPC-1	33	0	0	0	0
1	AEPC-1	20	16	16	15	47
1	AEPC-3	20	20	20	20	60



(a) TEPC-1



(b) AEPC-1



(c) AEPC-3

Fig. 11: Waveforms for setups TEPC-1, AEPC1 and AEPC-3

IV. CONCLUSION, DISCUSSION AND FUTURE WORK

The novel solution for extracting the ICG fiducial points to calculate the cardiac efficiency (CO and SV) -as well as on the block diagram level and as an implementation example in schematics- has been proposed, discussed and analyzed. This work shows, that it is possible and reasonable to embed the solution of the ICG-parameter estimation into the wearable device and also into the dedicated chip. Of course, more signals are needed for testing this solution, to improve their validation.

If compared to classical solutions, with ADC and digital processor analyzing the waveforms, the power consumption of the solution, if implemented in low-power CMOS ASIC, will be by an order less. For example the very low-power microcontroller MSP430 is consuming in active mode at least 400 μA and a 16-bit low power ADC ADS-1118 at least 100 μA , so totally more than 0.5 mA, then commercial low-power op-amps can work at few μA -s (e.g. LTC6258 takes 20 μA at 1 MHz bandwidth) and custom-design ones work even at lower consumption. Also digital CMOS counters, having a fractional complexity of microcontrollers and microprocessors can be easily implemented with extremely small power consumption.

From the accuracy viewpoint of the measurement electronics - the proposed solution can have the same accuracy, as digital implementation with high resolution (16-bit or more) ADC with relatively high sample-rate (in the context of the very low-power electronics, e.g. of 1 kHz) with sophisticated digital signal processing, replaced now by processing of few samples per second, latched precisely in analog domain. Also, as analog values of the fiducial points (especially critical is the C-point amplitude value, defining very much the estimation of the cardiac SV and CO values) are latched asynchronously, not sampled on the grid of the ADC sample-rate, the measurement accuracy will be significantly improved.

As a discussion, an important aspect is the chosen concept for the acquisition of interesting bio-signal - the choice of suitable location for placement of electrodes to the measurement accuracy of the ICG parameters, starting from the fiducial points, their locations in time and amplitudes.

REFERENCES

- [1] O. G. Martinsen and S. Grimnes, *Bioimpedance and Bioelectricity Basics*, 3rd ed. Academic Press, Aug 2014.
- [2] R. P. Patterson, "Fundamentals of impedance cardiography," *IEEE Engineering in Medicine and Biology Magazine*, vol. 8, no. 1, pp. 35–38, 1989.
- [3] M. Nabian, Y. Yin, J. Wormwood, K. S. Quigley, L. F. Barrett, and S. Ostadabbas, "An open-source feature extraction tool for the analysis of peripheral physiological data," *IEEE Journal of Translational Engineering in Health and Medicine*, vol. 6, pp. 1–11, 2018.
- [4] H. Yazdani, A. Mahnam, M. Edrisi, and M. Esfahani, "Design and implementation of a portable impedance cardiography system for noninvasive stroke volume monitoring," *Journal of Medical Signals and Sensors*, vol. 6, pp. 47–56, Jan 2016.
- [5] E. Piuze, S. Pisa, E. Pittella, L. Podestà, and S. Sangiovanni, "Wearable belt with built-in textile electrodes for cardio—respiratory monitoring," *Sensors*, vol. 20, no. 16, 2020.
- [6] J. Xu, X. Gao, A. Lee, S. Yamada, E. Yavari, V. Lubecke, and O. Boric-Lubecke, "Wrist-worn heartbeat monitoring system based on bio-impedance analysis," *2016 38th Annual International Conference of the IEEE Engineering in Medicine and Biology Society (EMBC)*, pp. 6294–6297, 2016.
- [7] M. Metshein, P. Annus, R. Land, M. Min, and A. Aabloo, "Availability and variations of cardiac activity in the case of measuring the bioimpedance of wrist," in *2018 IEEE International Instrumentation and Measurement Technology Conference (I2MTC)*, 2018, pp. 1–5.
- [8] K. Pesti, M. Metshein, P. Annus, H. Kõiv, and M. Min, "Electrode placement strategies for the measurement of radial artery bioimpedance: Simulations and experiments," *IEEE Transactions on Instrumentation and Measurement*, vol. 70, pp. 1–10, 2021.
- [9] J. C. Miller and S. M. Horvath, "Impedance cardiography," *Psychophysiology*, vol. 15, no. 1, pp. 80–91, 1978.
- [10] J. Bour and J. Kellett, "Impedance cardiography - a rapid and cost-effective screening tool for cardiac disease," *European journal of internal medicine*, vol. 19, pp. 399–405, Nov 2008.
- [11] S. M. M. Naidu, U. R. Bagal, P. C. Pandey, S. Hardas, and N. D. Khambete, "Detection of characteristic points of impedance cardiogram and validation using doppler echocardiography," in *2014 Annual IEEE India Conference (INDICON)*, 2014, pp. 1–6.
- [12] K. Dhemman, P. Mayer, M. Magno, and S. Schuerle, "Wireless, artefact aware impedance sensor node for continuous bio-impedance monitoring," *IEEE Transactions on Biomedical Circuits and Systems*, vol. 14, no. 5, pp. 1122–1134, 2020.
- [13] S. Weyer, T. Menden, L. Leicht, S. Leonhardt, and T. Wartzek, "Development of a wearable multi-frequency impedance cardiography device," *Journal of Medical Engineering & Technology*, vol. 39, pp. 1–7, Jan 2015.
- [14] M. Min, O. Martens, and T. Parve, "Lock-in measurement of bio-impedance variations," *Measurement*, vol. 27, pp. 21–28, Jan 2000.
- [15] M. Metshein, T. Parve, P. Annus, M. Rist, and M. Min, "Realization and evaluation of the device for measuring the impedance of human body for detecting the respiratory and heart rate," *Elektronika ir Elektrotechnika*, vol. 23, pp. 36–42, June 2017.
- [16] G. Roa, T. Le Pelleter, A. Bonvilain, A. Chagoya, and L. Fesquet, "Designing ultra-low power systems with non-uniform sampling and event-driven logic," in *2014 27th Symposium on Integrated Circuits and Systems Design (SBCCI)*, 2014, pp. 1–6.
- [17] M. Greitans, R. Shavelis, L. Fesquet, and T. Beyrouthy, "Combined peak and level-crossing sampling scheme," in *9th International Conference on Sampling Theory and Applications (SampTA'11)*, Singapore, Singapore, May 2011, pp. Fr2S12.1 – P0158.
- [18] B. Sramek, "Noninvasive continuous cardiac output monitor," U.S. Patent 4 450 527, May 22, 1984.
- [19] S. Mandal and S. Dasgupta, "Modified cmos peak detector and sample hold circuit for biomedical applications," in *2018 Conference on Emerging Devices and Smart Systems (ICEDSS)*, 2018, pp. 113–116.
- [20] K. Achtenberg, J. Mikołajczyk, D. Szabra, A. Prokopiuk, and Z. Bielecki, "Review of peak signal detection methods in nanosecond pulses monitoring," *Metrology and Measurement Systems*, vol. 27, no. 2, pp. 203–218, 2020.
- [21] W. Reklewski, K. Heryan, M. Miśkiewicz, and P. Augustyniak, "Real time eeg r-peak detection by extremum sampling," in *2020 6th International Conference on Event-Based Control, Communication, and Signal Processing (EBCSCP)*, 2020, pp. 1–7.
- [22] S. Benouar, A. Hafid, M. Attari, M. Kedir-Talha, and F. Seoane, "Systematic variability in icg recordings results in icg complex subtypes - steps towards the enhancement of icg characterization," *Journal of electrical bioimpedance*, vol. 9, no. 1, p. 72–82, January 2018. [Online]. Available: <https://europepmc.org/articles/PMC7852018>
- [23] S. M. M. Naidu, P. C. Pandey, and V. K. Pandey, "Automatic detection of characteristic points in impedance cardiogram," in *2011 Computing in Cardiology*, 2011, pp. 497–500.
- [24] M. Metshein, A. Gautier, B. Larras, A. Frappe, D. John, B. Cardiff, P. Annus, R. Land, and O. Martens, "Study of electrode locations for joint acquisition of impedance- and electro-cardiography signals," in *2021 43rd Annual International Conference of the IEEE Engineering in Medicine Biology Society (EMBC)*, 2021, pp. 7264–7267.